



# A FINITE ELEMENT ANALYSIS OF SUBSTATION ALUMINUM BUSBARS

[ME 6124] FINITE ELEMENT METHOD FINAL PROJECT

SAMEER ZAHEER, RYAN GRAJEWSKI, & GREY WILLIAMS

GEORGIA INSTITUTE OF TECHNOLOGY



# Contents

<b>Introduction</b> .....	2
<b>Objectives</b> .....	2
<b>Modeling</b> .....	3
Geometry .....	3
<b>Material Properties</b> .....	4
<b>Loading Conditions</b> .....	5
<b>Analysis</b> .....	5
Analysis Type Using Ansys.....	5
Model Type .....	6
Element Selection .....	6
Boundary Conditions.....	6
Mesh Convergence Studies.....	7
<b>Results</b> .....	8
<b>Flat Bar Analysis</b> .....	8
<b>Angle Bar</b> .....	9
<b>Tubing</b> .....	10
<b>Integral Web Bar</b> .....	11
Discussion of Results.....	12
Validation of Results .....	<b>Error! Bookmark not defined.</b>
Additional Studies .....	14
Objective .....	14
Changes from Previous Study .....	14
Results.....	15
Future Work.....	<b>Error! Bookmark not defined.</b>
Conclusions .....	15
<b>Appendix A</b> .....	17
Tabulated material property values for 6061 Aluminum Alloy. ....	17
<b>References</b> .....	19

## Introduction

In the electric utility industry, dedicated facilities known as substations house equipment for transforming electricity between voltages, sectionalizing the electrical grid, and monitoring power flow. Within substations, rigid aluminum conductors are commonly used as the central “bus” from which other circuits branch. Ensuring the continual operation of these aluminum busbars is a crucial engineering design problem for power companies as they are integral to powering nearly all other societal functions.

As shown in Figure 1, busbars are typically installed in open air environments. Therefore, they must be designed to withstand the forces arising from the local climate, namely, ambient temperatures. Internally, these aluminum conductors also experience joule heating resulting from their inherent electrical resistance. This effect is often amplified on hot days when air conditioner use increases electrical demand.

On cold days, much of communities’ heating demands are met using natural gas, reducing electrical demand. This makes winter the preferred time to perform grid maintenance as electrical loads may be diverted without overloading circuits. Hence, conductors are often rigidly installed at their coldest internal temperatures and expand/contract against their supports as they heat and cool throughout the year. Thus, an important design consideration is the thermal fatigue stresses which develop inside them.

Busbars are commercially available in a variety of standard cross-sections, including flat bar, angled bar (UABC), tubing, and integral web (IWCB). Each of these options present tradeoffs in terms of ampacity and structural strength. Considering the electrical loading conditions and environmental influences, perhaps the most important design consideration is the choice of busbar cross-sectional geometry. This report presents a finite element analysis of the geometry effects of different busbars as they relate to material deformation and fatigue life.



*Figure 1: Example substation facility*

## Objectives

The objective of this study was to analyze the fatigue life of four common aluminum busbar conductors undergoing cyclic thermal expansion/contraction resulting from changing ambient temperatures and electrical load. The four busbar types analyzed were rectangular (flat) bar, angle, tube, and integral web. Finite element analysis software ANSYS was used to model the heat generation, heat dissipation, deformation, stress, and fatigue life of each busbar type. Assumptions and validation were

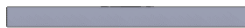

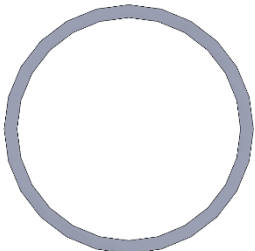
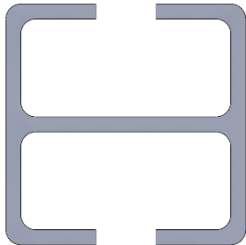
informed by the design standards of Southern Company, a large electric utility serving much of the southeastern United States. Where feasible, models were also validated with analytical solutions. The results are to be compared to existing standards and provide insight into standard accuracy and allow for revisions.

## Modeling

### Geometry

Busbar cross-sections analyzed in this study are shown in Table 1. The dimensions for these cross-sections are considered standard in the electric utility industry, and come readily available from manufacturers in lengths of 10 ft, 16 ft, and 42 ft. For consistency of comparison, each busbar's 3D model used for FEA simulation is 10 feet long. Shown in Figure 2, two 5/8" diameter bolt holes are placed on either side of each busbar so they may be mounted to their supporting porcelain insulators. *These holes are spaced to make use of Saint-Venant's Principle.* The tubing busbar does not have bolt holes, however, because end-clamps are used instead to mount in them in position. This style support is shown in Figure 3.

Table 1: Profiles of Busbar Cross-Sections and their Geometry

 Flat (Rectangular) Bar	 Angle (UABC)	 Tubing	 Integral Web (IWCB)
<b>Dimensions [in]</b>			
$\frac{3}{8}'' \times 4''$	$4'' \times 4'' \times \frac{1}{4}''$	4" NPS Sch. 40 Tube (4.5" OD, 4.03" ID)	$4'' \times 4'' \times \frac{1}{4}''$
<b>Cross-Sectional Area [in<sup>2</sup>]</b>			
1.5	1.9375	3.1487	3.781
<b>Area Moment of Inertia [in<sup>4</sup>]</b>			
0.018	3.039	7.181	5.788
<b>Linear Resistance [<math>\mu\Omega</math>/ft]</b>			
12.566	9.729	5.987	4.985

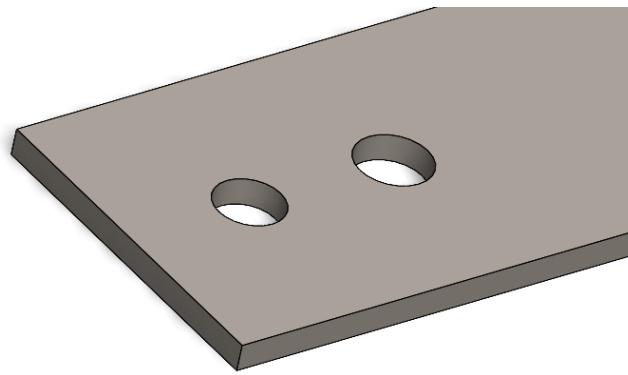


Figure 2: Example of the Flat Bar's 5/8" Bolt Holes used for mounting.

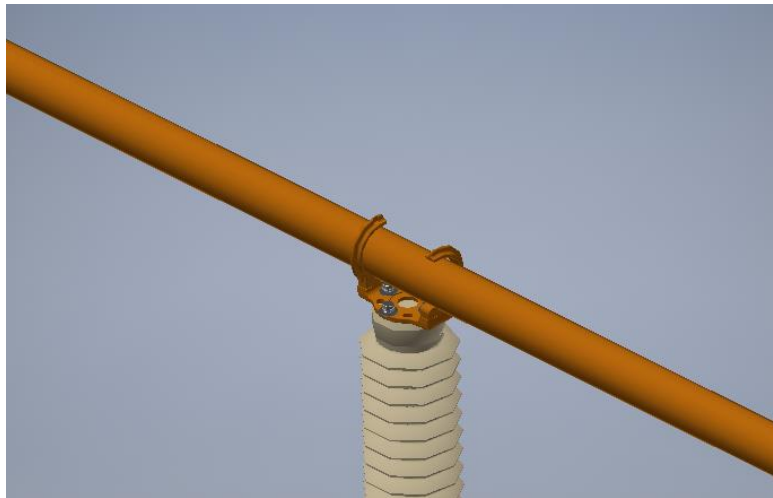


Figure 3: Example of tubing affixed to its support with a clamp.

### Material Properties

Each busbar is made of 6061 Aluminum Alloy with T6 temper. This material selection is consistent with Southern Company's design standards and is what they employ in all current substation construction. This material is preferred for its high strength-to-weight ratio, excellent corrosion resistance, and low resistivity. The material properties for 6061-T6 aluminum alloy are shown below in Table 2 – each of these values were obtained from the Engineering Data Log within ANSYS. ANSYS defines certain properties based on temperature level, so applicable properties are tabulated in Appendix A.

Table 2: Material Properties for 6061-T6 Aluminum Alloy

Property	Value
Density	2713 [lb/in <sup>3</sup> ]
Tensile Yield Strength	37594 [psi]
Tensile Ultimate Strength	45411 [psi]
Electrical Resistance	18.85 [ $\mu\Omega$ /in <sup>2</sup> /ft]
Specific Heat Capacity	0.214 [Btu/lb*°F]
Radiation Heat Emissivity	0.11
Young's Modulus	See Table A1 in Appendix A
Thermal Conductivity	See Table A2 in Appendix A
Coefficient of Thermal Expansion	See Table A3 in Appendix A

## Loading Conditions

Table 3 displays the loading conditions applied to each busbar. These conditions were informed by data published by Southern Company. In general, there were four types of loads applied in each simulation: the distributed gravitational weight of the busbar, a current running through the busbar, radiation heat loss and convection heat loss. This is in addition to setting up the installation temperature and operational ambient temperature.

To highlight differences between conductors, the worst-case scenario for each loading condition was assumed. At installation, conductors were assumed to have uniform internal temperatures of 32°F, assuming installation on a chilly day. At operation, the ambient temperature was assumed to be 120°F.

For periods of high electricity demand, a current of 2000 Amps was chosen to run through the bars. The amount of current flowing through a busbar can be modeled as a voltage change across the busbar. Using the linear resistance data from table 1 and multiplying by the length of each busbar, the total resistance value was obtained. Voltage drop across the busbar was calculated using the current and resistance values and Ohms Law. The voltage difference was applied in the analysis.

Table 3: Loading Conditions

Condition	Value
Installation Temperature	32°F
Operation Ambient Temperature	120°F
Current Load	2000 A

## Analysis

### Analysis Type Using Ansys

The problem contains electric and thermal loads on the busbar, which cause internal stress in rigidly mounted busbars. To consider all loads and boundary conditions, a Thermal-Electric analysis is paired with a Static Structural analysis.

Inputs for the Thermal-Electric analysis include ambient temperature, voltage difference across the busbar, and emissivity of 6061 Aluminum. These thermal boundary conditions are used to obtain the steady state temperature values of the busbar resulting from joule heating, convection, and radiation. The Static Structural analysis computes Von Mises stress and deformation of the busbar by using the initial installation temperature of the busbar at 32°F and the temperature data obtained from the Thermal-Electric analysis. Shown in Figure 4, the fatigue life is calculated by modeling a zero-based loading cycle of the thermal and static loading conditions where full load conditions are the output of the Static Structural Analysis.

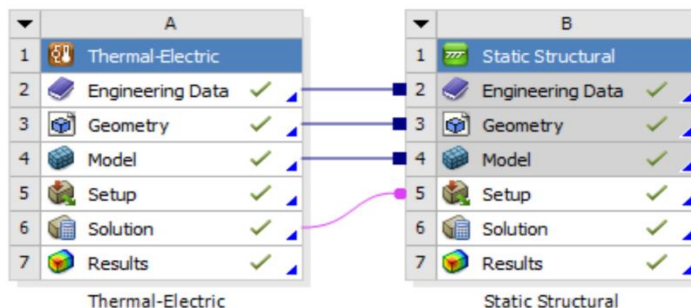


Figure 4: Ansys Mechanical Workbench Analysis Schematic

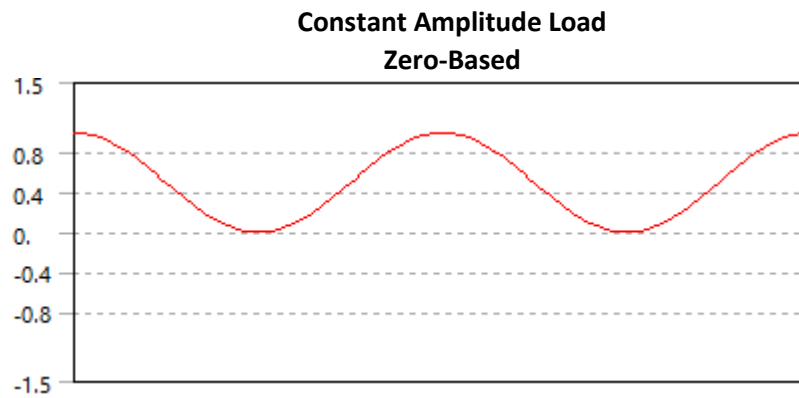


Figure 5: Ansys Zero-Based Loading Cycle Function

### Model Type

Most of the busbars are 3D in nature, therefore a 3D model was used to perform analysis of all busbars. The deformation, stress and temperature profiles of various busbars also vary in all 3 axes. Cross-sections such as the Angle busbar show deformation in multiple orthogonal directions to the axial direction, as shown later in the results section. While some busbars and boundary conditions can be modeled in 2D to reduce computing cost, this was not required for analysis' sake; therefore, a 3D model was used. To capture the behavior of smaller features on each bar, edge-sizing techniques were employed that decreased the size of each element to allow for a more accurate calculation. For each bolt-hole feature, the # of edge divisions was increased to 20.

### Element Selection

Element SOLID187 was chosen as the element type. Figure 5 shows a diagram of the element. According to the ANSYS element reference 'SOLID187 element is a higher order 3-D, 10-node element. SOLID187 has a quadratic displacement behavior and is well suited to modeling irregular meshes (such as those produced from various CAD/CAM systems).' This element has 10 nodes with 3 degrees of freedom per node. This is a typical element used for 3D analysis on ANSYS and requires. The element considers bending loads, axial and perpendicular loads and thus allows for a lower resolution mesh. This suits the requirements of our 3D analysis.

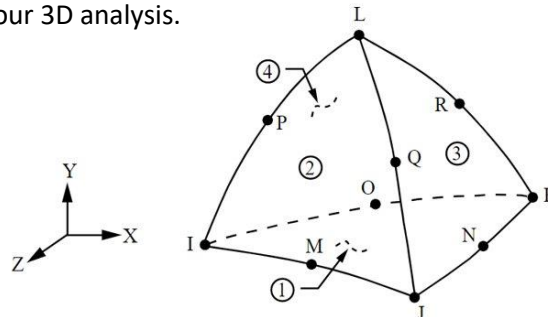


Figure 5: Element SOLID187 Diagram

### Boundary Conditions

Thermal and Mechanical boundary conditions are applied to models. A summary of these conditions can be seen in table 4.

Thermal convection as well as radiation boundary conditions are applied to all surfaces of the busbars exposed to the ambient environment. Convection was considered at exposed surfaces of the busbars, with a temperature varying convection coefficient. The coefficient data was preloaded from an

ANSYS library considering simplified convection with stagnant air. This is chosen as a worst-case scenario. All surfaces of the busbars along the axial direction have an applied convections boundary condition, expect the inner surface of the tube. Due to the large length of the tube relative to cross-sectional area, the air temperature in the internal section of the tube is assumed to be equal to the temperature of the inner surface of the tube. Thus, giving a zero-convection boundary condition at the internal surface of the tube.

Similarly, radiation boundary conditions are applied to all surfaces of the busbars exposed to the ambient environment. The emissivity of the material is 0.011 as shown in table 1 and is held constant with temperature. A zero-radiation boundary condition is applied to the internal surface of the tube, because it is not exposed to the ambient environment.

Mechanically all busbars have fixed support boundary conditions applied at the mounting holes. The tube busbar has fixed support boundary conditions applied at the surfaces perpendicular to the axial length direction. Since mounting holes are not used for tube busbars, they are held rigidly using clamps which are then mounted to the substation structure.

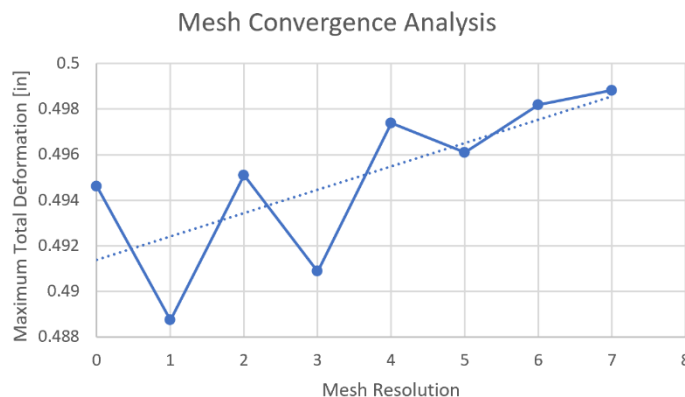
These boundary conditions represent rigidly mounted busbars, which are given no room for expansion, with low temperature dissipation using convection. Thus, these boundary conditions are chosen to induce the greatest temperature difference in busbars. This leads to the greatest internal stresses and thus allows for fatigue testing in the worst-case scenario.

*Table 4: Boundary Conditions*

Condition	Description
Convection	Temperature dependent convection coefficient for stagnant air applied on all exposed Surfaces.
Radiation	Emissivity = 0.11. Applied on all exposed surfaces.
Mechanical	Fixed supports at mounting holes.

### Mesh Convergence Studies

Figure 6 shows the maximum total deformation recorded for the rectangular bar as the mesh resolution is increased. As seen in the figure as the mesh resolution is increased, the value of the deformation has little change but starts to converge towards a value of 0.5. However, the change between the deformation values at the minimum and maximum resolution are not significant enough to set the mesh resolution to its maximum value. This could be attributed to ANSYS lowest resolution mesh being too fine to show convergence. To minimize computing time a mesh resolution of 2 was chosen.



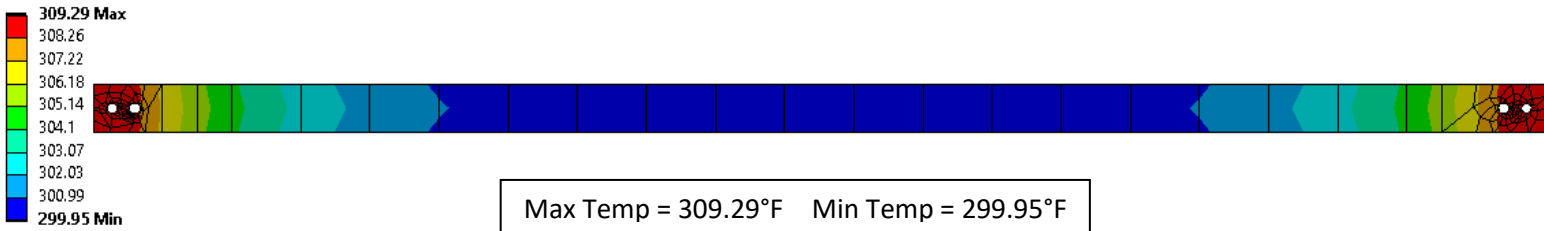
*Figure 6: Mesh Convergence Analysis*



# Results

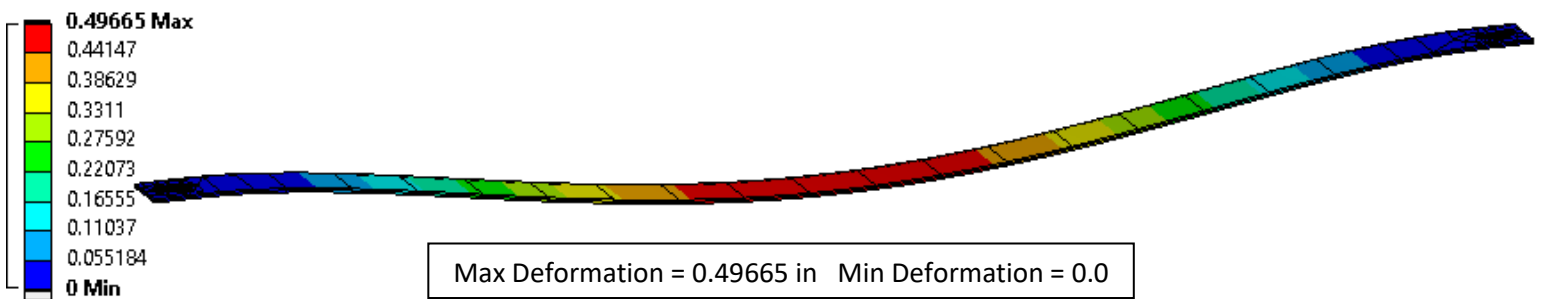
## Rectangular Bar Analysis

### Surface Temperature Distribution [°F]



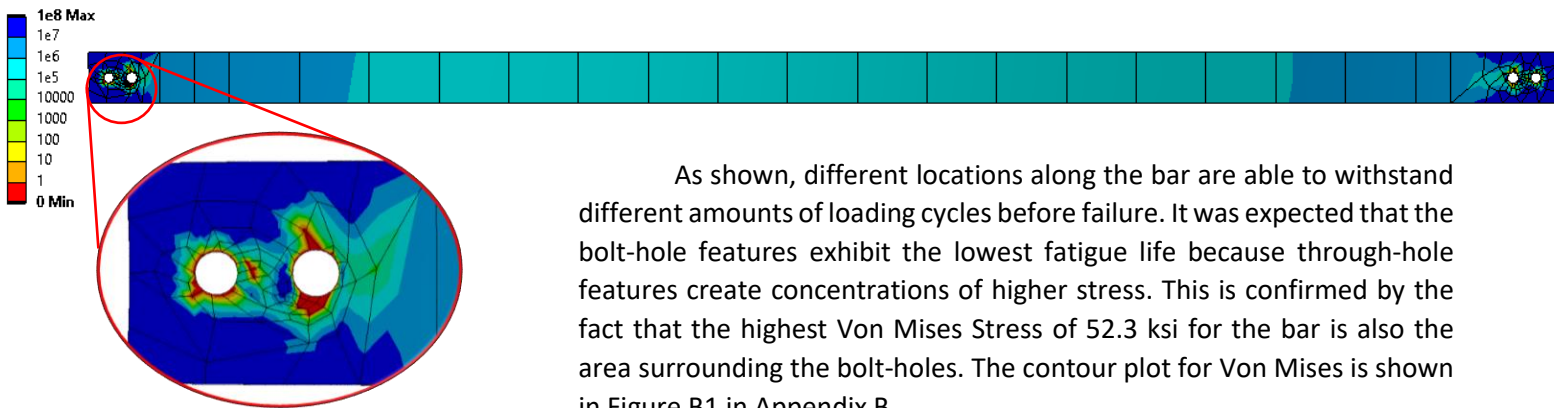
The location of the maximum temperature was found to be at either end of the Flat Bar. It is reasonable that the temperature is not uniformly distributed along the length of the bar as the bolt-hole features effectively remove cross-sectional area available for current to flow through. Thus, electrical resistance around these holes increases and consequently so does internal heat generation.

### Total Deformation [in]



It was expected that the flat bar bow downwards when deforming due to thermal expansion and gravitational weight of the bar itself. The Max and Min values shown above include deformation in all three directions. However, with a Z-Direction deformation of 0.49658 in, it is apparent that deformation in this direction is the leading influence. This is likely because the fixed-supports applied to the bolt-holes restrict axial deformation, and also due to the way Ansys applies the distributed gravitational weight of a body at its center.

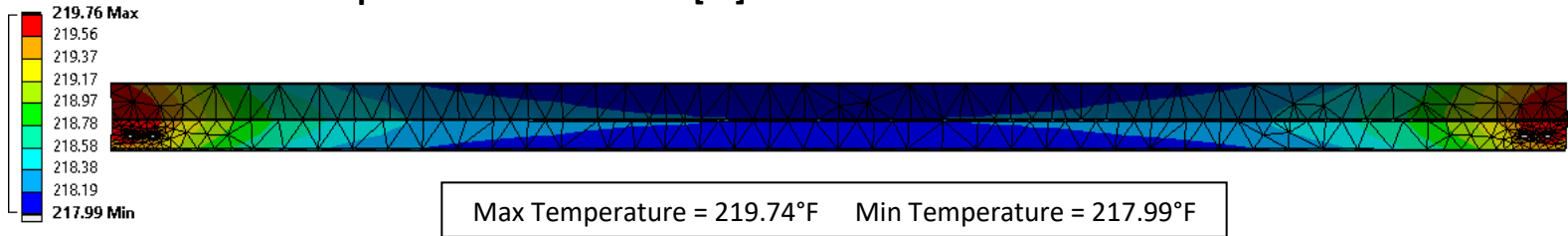
### Fatigue Life [# of Cycles Until Failure]



The fatigue life for the center portion of the bar is calculated as 10 million loading cycles. In comparison to other bars, this is notable as it does not reach the infinite life datum of 1e8 cycles. This is a reasonable result as the rectangular cross-section is very thin along the z-axis, making it more susceptible to bending and fatigue.

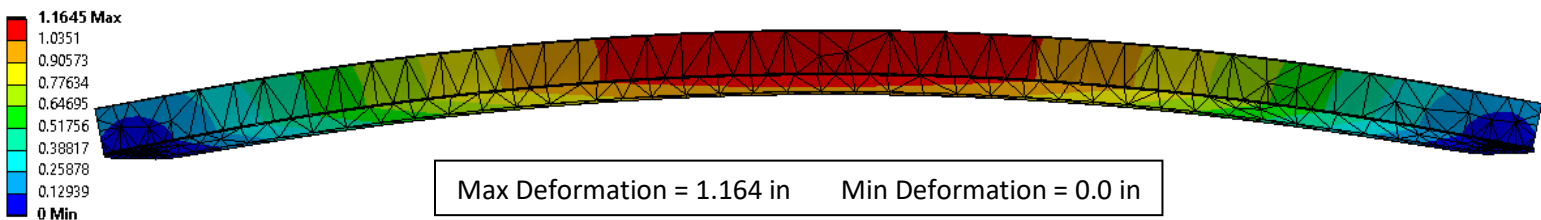
## Angle Bar

### Surface Temperature Distribution [°F]



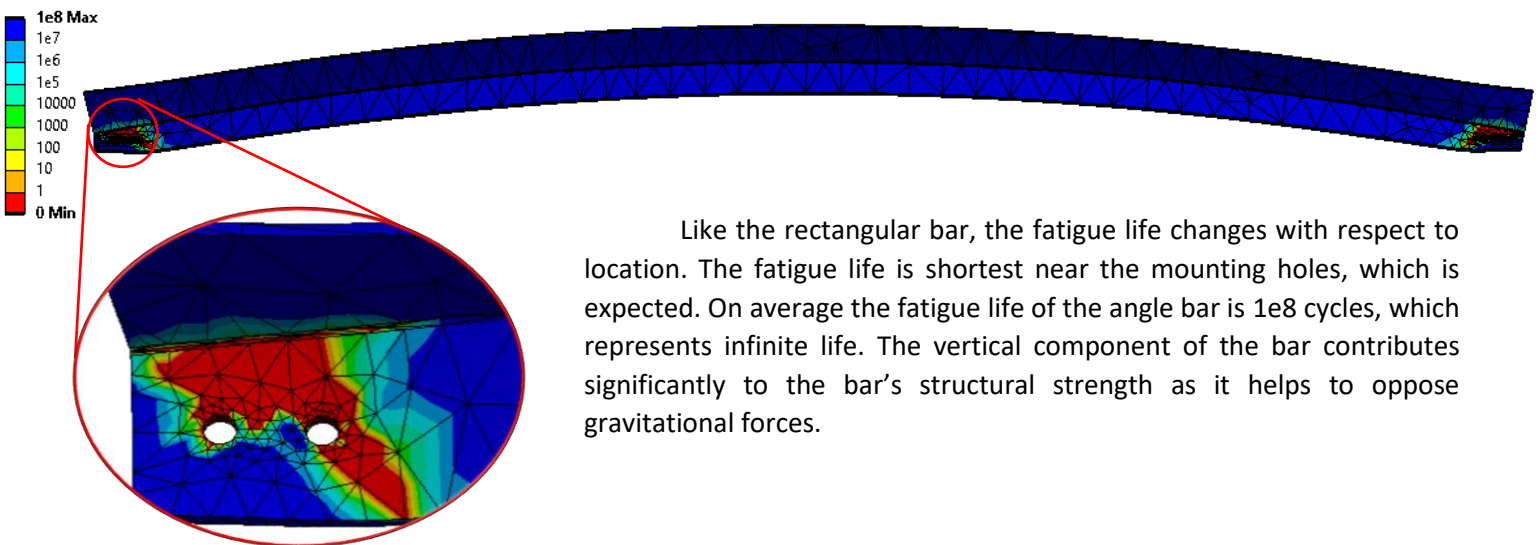
A similar analysis to the Flat Bar applies here for the location of highest temperature, as the Angle Bar also has bolt-hole features. However, the Angle Bar has a relatively large surface area because of its vertical component, allowing for greater heat transfer by convection. Since the ambient temperature is colder than the bar, this convection removes heat from the bar and leads to a lower maximum temperature of 219.76°F.

### Total Deformation [in]



The total deformation of the Angle Bar demonstrates how the cross-sectional geometry impacts busbar behavior. Despite being a simply supported beam with its weight applied to its center, the Angle Bar deforms upwards against gravity. The thermal expansion of the vertical component of the bar drives this behavior.

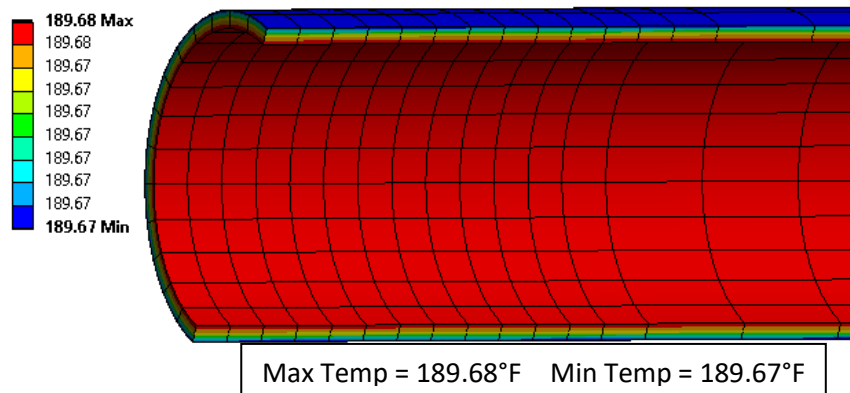
### Fatigue Life [# of Cycles Until Failure]



Like the rectangular bar, the fatigue life changes with respect to location. The fatigue life is shortest near the mounting holes, which is expected. On average the fatigue life of the angle bar is 1e8 cycles, which represents infinite life. The vertical component of the bar contributes significantly to the bar's structural strength as it helps to oppose gravitational forces.

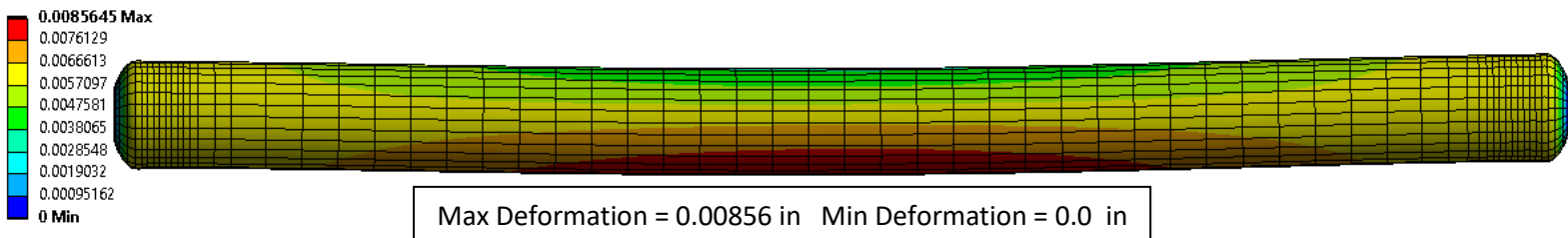
## Tubing

### Surface Temperature Distribution [°F]



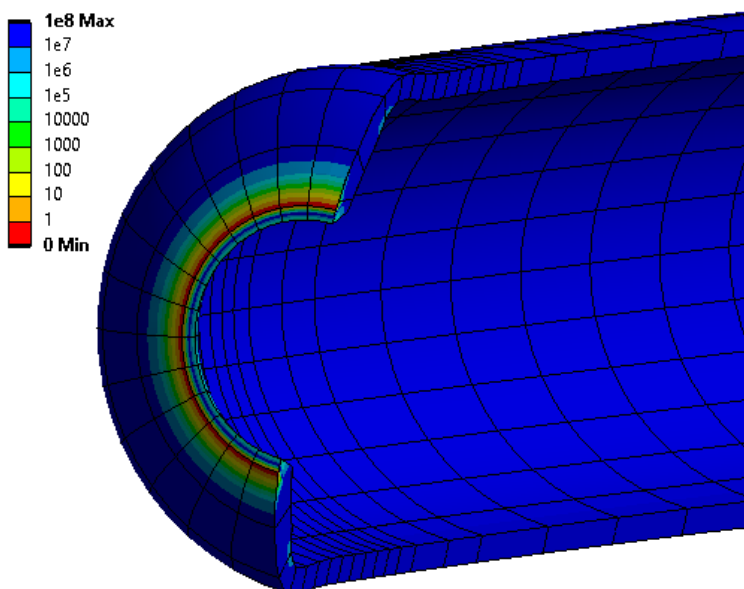
The tubing exhibits the lowest temperature of all busbars with a maximum of 189.68°F. The temperature difference is relatively small between outer and inner surfaces as the tube, this is due to the small thickness and high conductivity of the tube. The temperature difference is relatively small between outer and inner surfaces as the tube, this is due to the small thickness and high conductivity of the tube. The internal temperature is higher, because there is no convection on the inside of the tube.

### Total Deformation [in]



The total deformation shows the tube bending downwards, due to gravity and the increase in temperature. The bar also expands radially due to the thermal loading. Though exaggerated on this contour plot, the deformation of the tube is very low comparatively.

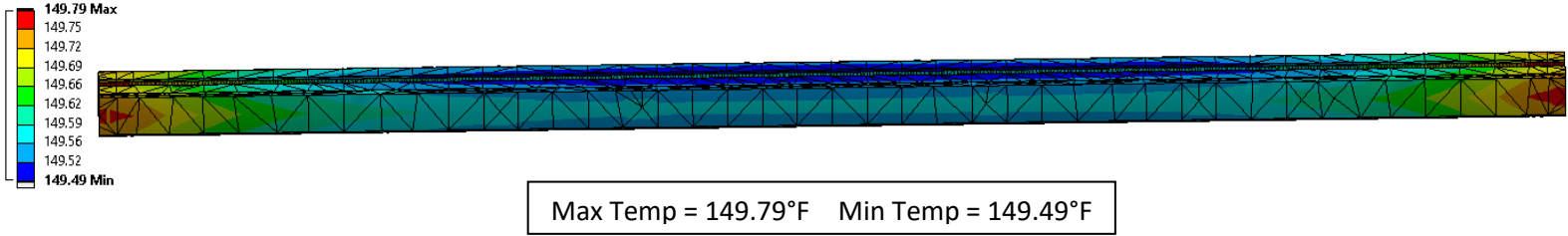
### Fatigue Life [# of Cycles Until Failure]



Like the fatigue of previous busbars, the tube has infinite life over a majority of its surface. The lower fatigue life near the edge is due to the fixed support boundary condition applied there.

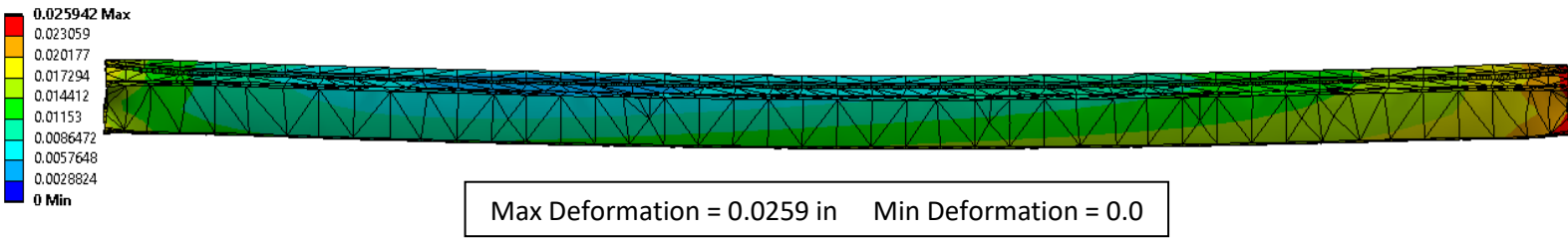
# Integral Web Bar

## Surface Temperature Distribution [°F]



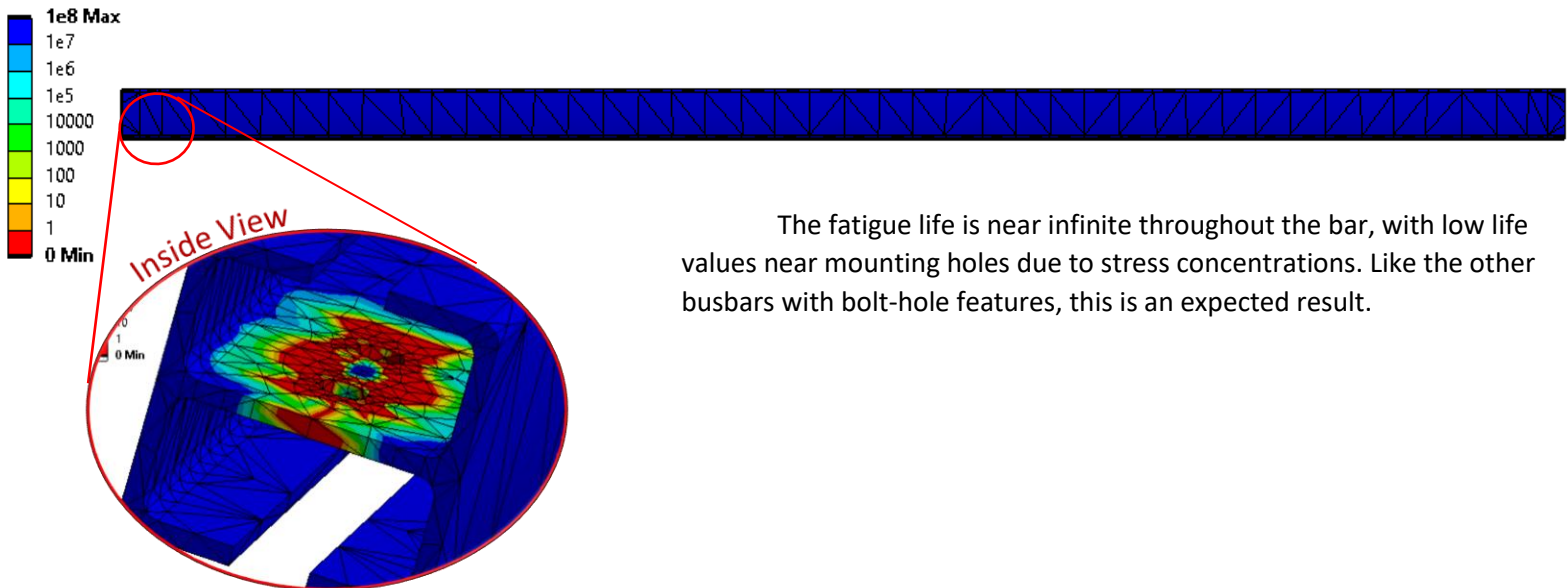
The surface temperature profile of the Web bar matches previous profiles, with higher temperature around the edges. Because there are inner channels open to the ambient, there is greater surface area available for convection.

## Total Deformation [in]



Similar to the tube and the rectangular bar, the Integral Web bar bends downwards due to the temperature increase and gravity. The unique geometry of the Integral Web around the bolt-hole features also forces greater deformation at the edges of the bar.

## Fatigue Life [# of Cycles Until Failure]



## Discussion of Results

In summary of these results, Table 7 displays all key datapoints calculated for each bar. Under the thermal and static structural loading conditions, the Angle Bar, Tubing, and Integral Web all demonstrated a significant longevity. In contrast, the Rectangular Bar was only able to withstand  $1e7$  loading cycles. This is not surprising, however, as the rectangular cross-section is notably thinner in the Z-direction than all other bars, making it more susceptible to gravitational pull and extraneous forces applied to its center. In total, the fatigue life values for each bar satisfactorily validate Southern Company's design standards that each bar be in continual operation under normal conditions for a lifespan of 50 years [1].

For heat generation and temperature distribution of each bar, there is a noticeable trend between maximum temperature and surface area of the busbar. The busbars with the greatest surface areas are able to give more off heat via convection to the surrounding environment. Joule heating also had the greatest influence on maximum temperature near areas of through-hole features, demonstrating the relationship between cross-sectional area and electrical resistivity. The tubing bar is perhaps the busbar that performed the best in terms of minimal deformation and low temperatures. This fact accurately mimics real substation design, as tubing busbars are commonly used as the central, longest busbars that span the entire facility and require the longest continual operation. Ultimately, demonstrating lower temperature values is more advantageous as a higher temperature of the busbar contributes to higher electrical resistance.

Furthermore, one of Southern Company's design criteria states that busbars should be designed with the expectation that, in a worst-case scenario, the busbar itself be roughly  $212^{\circ}\text{F}$  hotter than the surrounding ambient temperature [1]. The rectangular bar is the only conductor option that does not fall within that design standard, exhibiting a maximum temperature difference of  $277.29^{\circ}\text{F}$  greater than ambient. One feature that perhaps validates the rectangular bar's exaggerated behavior is the fact that these bars are typically used as short lifespan connecting bars in locations that require frequent repair.

*Table 7: Comparison of Busbar Results*

Busbar	Maximum Temperature [ $^{\circ}\text{F}$ ]	Maximum Total Deformation [in]	Average Fatigue Life [Cycles]
Rectangular Bar	309.29	0.4966	$1e7$
Angle Bar	$219.74^{\circ}\text{F}$	1.1645	$1e8$
Tubing	189.68	0.0085	$1e8$
Integral Web	149.79	0.0259	$1e8$

## Validation of Results

To validate the steady state temperatures of the conductors, analytical solutions were calculated for the cross-sections for which such solutions exist, namely the flat bar and tube. To do so, the temperatures of the conductors were solved for algebraically using the energy balance equation below. Results of these calculations can be found in Table 5 and can be seen to be with a few percent of the results obtained with FEA. This yields high confidence in all FEA results.

$$Q_{gen} = Q_{rad} + Q_{conv}$$

Where

$$Q_{gen} = I^2 R$$

$$Q_{rad} = \varepsilon \sigma A (T_{bus} - T_{amb})$$

$$Q_{conv} = \begin{cases} (h_{Top} A_{Top} + h_{Bottom} A_{Bottom} + 2h_{Side} A_{Side})(T_{bus} - T_{amb}) & \text{For bar} \\ hA(T_{bus} - T_{amb}) & \text{For tubing} \end{cases}$$

Hence,

$$T_{bus} = \begin{cases} \frac{I^2 R}{A_{Top}(2\varepsilon\sigma + h_{Top} + h_{Bottom}) + 2A_{Side}(\varepsilon\sigma + h_{Side})} & \text{For bar} \\ \frac{I^2 R}{A(\varepsilon\sigma + h)} & \text{For tubing} \end{cases}$$

Where

Current,  $I = 2000 \text{ A}$

Resistance,  $R = \begin{cases} 12.566 * 10^{-5} \Omega & \text{For bar} \\ 5.987 * 10^{-5} \Omega & \text{For tubing} \end{cases}$

Emissivity,  $\varepsilon = 0.11$

Stefan-Boltzmann constant,  $\sigma = 5.670374419 * 10^{-8}$

Exterior surface Area,  $A = \begin{cases} A_{Top} = 0.3096768 \text{ m}^2 \\ A_{Bottom} = 0.3096768 \text{ m}^2 \\ A_{Side} = 0.0290322 \text{ m}^2 \end{cases} \begin{matrix} \text{For bar} \\ \\ \text{For tubing} \end{matrix}$

Convection Heat Transfer Coefficient,  $h = \begin{cases} h_{Top} = 8.8 \frac{W}{\text{m}^2 K} \\ h_{Bottom} = 4.4 \frac{W}{\text{m}^2 K} \\ h_{Side} = 14.9 \frac{W}{\text{m}^2 K} \\ 5.2 \frac{W}{\text{m}^2 K} \end{cases} \begin{matrix} \text{For bar} \\ \\ \\ \text{For tubing} \end{matrix}$

*Table 5: Analytical Results of Steady State Temperature  
(Uniform temperature distribution assumed)*

<b>Busbar</b>	<b>Steady State Temperature</b>	<b>% Difference from FEA</b>
3/8" x 4" Rectangular Bar	302.87 °F	-2.07%
4" NPS, Sch. 80 Tubing	195.94 °F	3.30%

A secondary validation of these temperatures was made by comparing them to Southern Company design standards to ensure the temperatures fall within the conservative criteria. This criterion stipulates that, for 120°F ambient temperatures, conductors are sized to never exceed 245°F [1]. As a result of this standard, ampacities are assigned for each conductor type as shown in Table 6. From Table 6, it can be seen that the only conductor which fails the temperature requirement is also the one whose ampacity limits were exceeded in the analysis. Hence, the FEA results align with the implications of Southern Company Standards, which are themselves based upon theoretical analysis and real-world testing.

*Table 6: Southern Company Standards versus FEA Results*

<b>Busbar</b>	<b>Southern Company Temperature Limit [1]</b>	<b>FEA Steady State Temperature</b>	<b>Southern Company Ampacity Limits [1]</b>	<b>FEA Applied Current</b>
3/8" x 4" Rectangular Bar	245°F	309.29°F	1780 A	2000 A
4" x 4" x 1/4" UABC		219.76°F	2564 A	
4" NPS, Sch. 80 Tubing		189.68°F	3248 A	
4" x 4" x 1/4" IWCB		149.79°F	4041 A	

## Additional Studies

### Objective

Additional analysis was done on busbars, simulating the busbars being mounted on slots that allow the busbars to move in the axial direction, along their length. This reduces the internal stresses, which reduces the risk of injury during maintenance when the tension or compression in the busbars is released. However, the deformation in the axial direction is required to be less than 3/8" to avoid collision with other components, which would entail additional design work and cost to allow for a higher deformation. The goal of this study is to determine which busbar shape minimizes its deformation in the axial direction and is best suited under these design goals.

### Changes from Previous Study

To simulate the study mechanical boundary conditions were modified. Fixed support boundary conditions are still applied to one side of the busbar, while the other side is restricted in all degrees of freedom except movement along the axial direction. This is done using the 'remote displacement' boundary condition in ANSYS. All other boundary and load conditions are held constant with respect to the previous study.

## Results

Table 8 below shows the maximum deformation in the axial direction by shape type. As seen in the table all busbars achieve a maximum deformation of less than 3/8 or 0.375 inches, except the rectangular bar. While the minimum deformation is achieved by the angle bar. This study reveals that even for spans of 10 feet, a non-rigidly mounted rectangular bar is not well suited. The deformation increases with the span therefore these results simply show the relation of the deformation of busbars with respect to one another.

*Table 8: Additional Study Table*

Busbar	Deformation in Busbar Axial Direction [in]
Rectangular Bar	2.8535
Angle Bar	0.001134
Tubing	0.29803
Integral Web	0.1841

## Future Work

Potential future work includes topology optimization of the cross-section of the busbar. The goal is to minimize the temperature change while keeping the load and boundary conditions constant. The temperature change depends on heat generation and heat dissipation of busbar. The heat generation through joule heating is dependent on the cross-sectional area, while the heat dissipation through convection is dependent on surface area. Therefore, the topology optimization would work to reduce cross-sectional area, while maximizing the surface area, which is the perimeter in the 2D busbar shape. The results could produce thin, rough surfaces which lead to high surface area, while keeping the cross-sectional area low. The shape produced by the optimization could be used to adjust busbar designs in the future.

## Conclusions

While some simplifying assumptions were made, the analysis appears to mirror what expected from analytical solutions as well as utility industry practice. Conductor cross-sectional area played the largest role in determining temperature change, deformation, and fatigue life on the bulk of the conductors. However, because if one part of the conductor fails, it all fails, fatigue life was most impacted by the means with which it was attached to its support structure. The presence of bolt holes seemed to be a much larger source of stress concentration than did the cross section of each conductor.

Likely, the use of washers in conjunction with the bolts will lessen this effect significantly by spreading the force required to fix the conductors in place over a larger area. Beyond this, fatigue life correlated closely with cross-sectional area as the larger areas yielded less heat generation and, in general, greater heat loss through convection and radiation. This effect was so prevalent in fact that despite the IWCB's shape stifling the free flow of natural convection, it was still able to maintain the lowest steady state temperature.

As a final note on practicality, the difference in performance of these conductors can be negligible at lower electrical loads. Though the IWCB performed the "best" of the conductors analyzed, its relatively



sharp corners can increase coronal discharge along the bus, reducing transmission efficiency. The round tube is much less susceptible to this but requires additional hardware and clamps to affix it to support structures, driving up material and installation costs. As such, it is most common to see tubing only on higher voltage applications ( $>115\text{kV}$ ). In application where voltages and loads are  $<25\text{kV}$  and  $<2000\text{A}$  respectively, bar and angle conductors are often preferred for their ease of use.

## Appendix A

Tabulated material property values for 6061 Aluminum Alloy.

*Table A1: Young's Modulus*

Temperature (C)	Young's Modulus (psi)
-270.1	11109890.71
-184.6	10961952.22
-99.04	10613861.65
-13.48	10194702.59
72.07	9768291.636
157.6	9330277.668
243.2	8815393.699
328.7	8091655.388
414.3	6958910.656
499.9	5158992.331

*Table A2: Thermal Conductivity*

Temperature (C)	Thermal Conductivity (BTU/(ft <sup>2</sup> hr (F/ft)))
-260.2	10.84506284
-172.4	56.70402062
-84.59	77.01901314
3.183	87.93918829
90.96	95.79709211
178.7	101.6327413
266.5	105.0416848
354.3	106.0817015
442.1	104.6950126
529.9	100.9393968

*Table A3: Coeff. Of Thermal Expansion*

Temperature (C)	Coefficient of Thermal Expansion (C <sup>-1</sup> )
-250.2	1.50E-05
-187.9	1.84E-05
-125.7	2.05E-05
-63.48	2.18E-05
-1.261	2.26E-05
60.96	2.31E-05
123.2	2.37E-05
185.4	2.44E-05
247.6	2.50E-05
309.9	2.55E-05

## References

- [1] Southern Company Services, *Substation Design Criteria Manual, Bus Design Methods*, 2019.